PREVENTION AND CONTROL OF VACUUM INTERVAL BY MANAGED PRESSURE INJECTION IN CEMENTING

by

Jiasheng FU[a,b*], Wei LIU[a,b], Xiaosong HAN[c], Qing ZHAO[a,b], Weiwei HAO[a,b], and Ning LI[c]

[a] CNPC Engineering Technology R&D Company Limited, Beijing, China
[b] National Engineering Research Center for Oil and Gas Drilling and Completion Technology, Beijing, China
[c] Key Laboratory for Symbol Computation and Knowledge Engineering of National Education Ministry, College of Computer Science and Technology, Jilin University, Changchun, China

Original scientific paper
https://doi.org/10.2298/TSCI2404397F

This article uses on-site drilling data and establishes a hydraulic model for pressure-controlled cementing to simulate and analyze the generation process of the vacuum interval in the wellbore, as well as the changes in the volume and height of the vacuum interval, bottom hole pressure, and point of interest pressure over time. This model can optimize and recommend key parameters such as target wellhead back pressure and displacement based on the pressure window and drilling parameters, with the target pressure of the focus point as the anchor point. Through the hydraulic model of controlled pressure cementing, the hydraulic parameters and processes of managed pressure cementing can be optimized and recommended, effectively ensuring the safety of the cementing process.

Key words: *managed pressure cementing, wellhead back pressure, vacuum interval, U-tube effect, hydraulic model*

Introduction

In the context of deep well cementing, the *U*-tube effect emerges as a crucial challenge, necessitating anexamination of the vacuum interval's formation and management. The *U*-tube effect signifies the imbalance between pressure within the drill pipe and the pressure within the annulus during the operation of the drilling system. The *U*-tube effect results from differing densities of cement slurry and drilling fluid in a wellbore. When this density difference surpasses a critical threshold, it creates a static pressure difference, overcoming flow resistance and initiating the *U*-tube effect [1]. This can lead to the formation of vacuum intervals within the wellbore. Notably, when engaging in activities such as connecting single pipes, tripping, logging, or conducting routine pump shutdowns, drilling fluid within the drill pipe continues to flow along the pipe and seeps into the annulus via the drill bit until equilibrium is established between the pressure within the drill pipe and the liquid column within the annulus [2, 3].

When a vacuum interval is generated, the standpipe pressure disappears, and the outlet flow and inlet flow continue to be imbalanced, affecting the complex judgment of the underground [4]. To address and mitigate the potential hazards associated with the *U*-tube effect, several strategies have been developed. These strategies encompass adjusting cement displace-

* Corresponding author, e-mail: fujsdr@cnpc.com.cn

ment procedures to alleviate the *U*-tube effect, employing bottom plugs during cementing, introducing friction between the bottom plug and the wellbore wall to counteract some of the effects stemming from fluid density differentials [5] and utilizing *U*-tube effect controllers [6-8].

Given the importance of managing vacuum intervals within the *U*-tube effect and addressing the associated hazards, it is essential to implement effective control measures. These measures may involve optimizing pumping rates [9, 10] managing cement slurry density differentials [11] or utilizing specialized *U*-tube effect controllers to minimize adverse impacts and ensure long-term well stability [12].This paper introduces a finely-tuned pressure control model that focuses on a precise pressure window to contain vacuum sections within the *U*-tube effect.

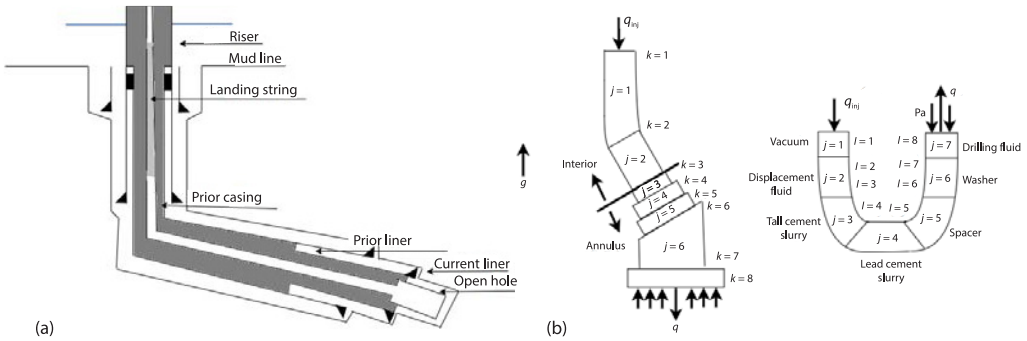

Figure 1. Standard well bore diagram and schematic representation of the well system; (a) standard wellbore diagram and (b) schematic representation of the well system

Methodology

A mathematical model is established by applying the principles of mass and momentum conservation analyze the fluid dynamics within the well during free fall. The field equations are simplified into a 1-D model through Eulerian area averaging [13]. The system of equations is further simplified into an ODE under the assumption that the system fluids exhibit incompressibility. The resultant initial value problem is addressed through numerical solutions employing the Runge-Kutta method.

Figure 1(a) shows a wellbore schematic used for model equations in directional wells with various system fluids, including drilling fluid, wash, spacer, lead cement slurry, tail cement slurry, and displacement fluid, with the *vacuum* interval considered a fluid, fig. 1(b). Fluid positions are shown in constant-diameter intervals along the *S* co-ordinate, starting at the column entrance, moving down the column, up the annulus, and ending at the annular exit.

At the wellhead, as pressure decreases, water vapor fills the low pressure zone, assuming incompressible fluids. Fluids are introduced at the vacuum/fluid interface, and the system treats pipe, wellbore, and borehole walls as rigid. Equation (1) defines the annular exit's boundary condition:

$$p_{k=8} = p_a \tag{1}$$

where p is the pressure and p_a – the annular pressure.

This condition holds throughout the entire process, with or without vacuum. The boundary conditions at the column entrance depend on the system's state. In the absence of vacuum and when the fluid column is not in free fall, the conditions are given [12]:

$$q = q_{\text{inj}} \tag{2}$$

and

$$\frac{\mathrm{d}q}{\mathrm{d}t} = \frac{\mathrm{d}q_{\mathrm{inj}}}{\mathrm{d}t} \tag{3}$$

where q and $\mathrm{d}q/\mathrm{d}t$ are flow rate and q_{inj} and $\mathrm{d}q_{\mathrm{in}}\mathrm{j}/\mathrm{d}t$ – the injection flow rate.

In the presence of a vacuum and with a free-falling column, the conditions reads:

$$p_{k=1} = p_v \tag{4}$$

where p_v is the internal pipe pressure.

To obtain the differential equations, a macroscopic balance is conducted utilizing the principles of mass and momentum conservation. Subsequently, during the free fall phase, we have [12]:

$$\frac{\mathrm{d}q}{\mathrm{d}t} = \frac{p_v - p_a + \sum_{j=1}^{7}\sum_{i=1}^{7}\left(\delta_j \rho_i \mathrm{g} h_{ij} + L_{ij}\left|\frac{\mathrm{d}p_f}{\mathrm{d}s}\right|_{ij}\right)}{\sum_{j=1}^{7}\sum_{i=1}^{7}\frac{\rho_i L_{ij}}{A_j}} \tag{5}$$

where δ and ρ are the density, g – the gravitational acceleration, h – the height, L – the segment length, A_j – the cross-sectional area, and $\mathrm{d}p/\mathrm{d}s$ – the pressure. Here, eq. (5) comprises a collection of terms in the numerator, representing contact and gravitational forces, and includes inertial terms in the denominator.

The pressures at each interface between intervals with constant diameters are provided, both in the presence and absence of a vacuum [12]. We may show [12]:

$$p_k = p_{k+1} + \sum_{i=2}^{7}\left[\rho_i\left(\frac{L_{ij}}{A_j}\frac{\mathrm{d}q}{\mathrm{d}t} + \delta_j \mathrm{g} h_{ij}\right) + L_{ij}\left|\frac{\mathrm{d}p_f}{\mathrm{d}s}\right|_{ij}\right] \tag{6}$$

where δ and ρ are density, g – the gravitational acceleration, h – the height, L – the segment length, A – the cross-sectional area, and $\mathrm{d}p/\mathrm{d}s$ – the pressure.

Friction loss terms calculated with Bingham, power-law, and Newtonian fluid equations, improved through Petrobras Research Center experiments.

Experiment

The purpose of this experiment was to systematically compare simulated environments under controlled pressure conditions with those lacking such control. The detailed results of this comprehensive comparative experiment are presented in fig. 2. For a thorough understanding of the experiment's parameters, extensive information is provided in tabs. 1-6 in the *Appendix*.

A comprehensive analysis of the experimental results clearly demonstrates that the method proposed in this study significantly prevents the formation of a vacuum interval. Figure 3 visually illustrates this effect: on the left side, results with controlled pressure are presented. When a denser drilling fluid follows a less dense drilling fluid, the formation of a vacuum interval within the wellbore becomes evident. Without pressure control, the vacuum interval does not dissipate immediately but persists for a specific duration asliquid injection continues. Concurrently, the hydrostatic pressure within the wellbore significantly decreases and, in certain scenarios, reaches absolute zero pressure.

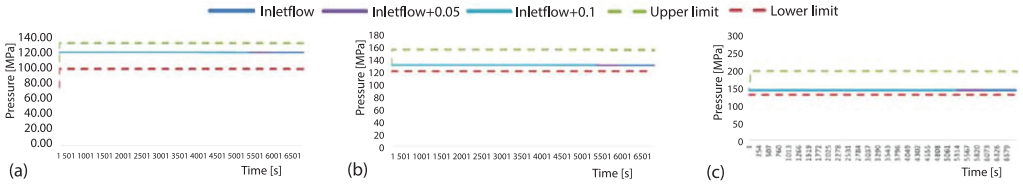

Figure 2. Comparison of fixed point pressure under different experimental conditions; (a) pressure at depth 5200, (b) pressure at depth 5700, and (c) pressure at depth 6300

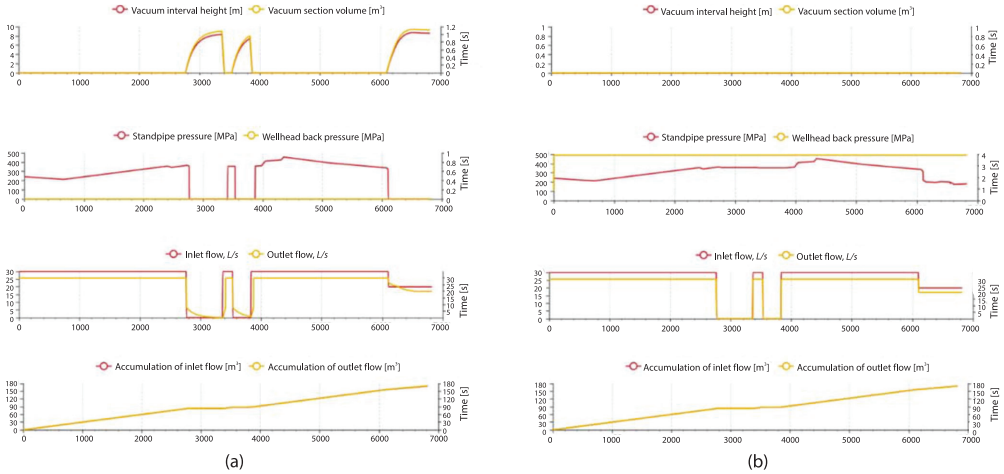

Figure 3. Experiments result comparison; (a) experiments without pressure management and (b) experiments with pressure management

Moreover, this article conducts a meticulous examination of the pressure variations at different flow rates, particularly under two distinct depths, as showcased in fig. 2. This analysis underscores the precision with which pressure can be controlled within the predefined upper and lower thresholds.

The software developed in the course of this study not only implements the underlying model but also furnishes a sophisticated virtual simulation environment, as exemplified in fig. 3. Within the software, users are merely required to input the essential parameters indispensable for the simulation of the environment through the intuitive menu bar on the right. Subsequently, they can initiate the calculation process by a simple click of the button. The software exhibits an inherent capability to autonomously compute and meticulously display a myriad of data acquired during the cementing process at the core of the interface. Furthermore, a simulated wellbore is artfully depicted on the left side of the software, affording a vivid and graphical representation of the intricate cementing process.

Conclusion

This research paper has addressed the critical issue of managing wellbore vacuum during cementing through pressure control. Wellbore vacuum can lead to fluctuations in bottom-hole pressure, affecting cementing quality and potentially causing well leakage in narrow pressure window formations. Addressing this issue holds significant potential value for enhancing operational efficiency, reducing safety risks, fostering technological innovation, and ensuring the quality of wellbores and cement sheaths in the oil and gas industry. These advan-

tages contribute to promoting sustainable exploration and production activities in the oil and gas sector.

Acknowledgment

This work is supported by the National Key RD Program Project of China (No. 2019YFA0708304), Project of CNPC (No. 2021DJ4103, No. 2020B-4019), and the Science and Technology Planning Project of Jilin Province (No. 20220201145GX).

Nomenclature

A – cross-sectional area, [m^2]
g – gravitational acceleration, [ms^{-2}]
h – height, [m]
q – flow rate, [m^{3}s^{-1}]
q_{inj} – injection flow rate, [m^{3}s^{-1}]
L – segment length [m]
p – pressure, [MPa]
p_a – annular pressure, [MPa]
p_v – internal pipe pressure, [MPa]

Greek symbol

ρ – density, [kgm^{-3}]

References

[1] Olve, E. R., *et a*l., Evaluation of MPD Methods for Compensation of Surge-And-Swab Pressures in Floating Drilling Operations, *Proceedings*, SPE/IADC Managed Pressure Drilling and Underbalanced Operations Conference and Exhibition, SPE 108346, Galveston, Tex., USA, 2007
[2] Liu, Y., Formation and Prevention of Vacuum Section in Casing During Cementing Process, *Oil Drilling Production Technology*, *11* (1989), 3, pp. 51-53
[3] Li, J., *et al.*, Study on U-Tube Effect in Deepwater Submarine Lifting Drilling System, *China Offshore Oil and Gas, 28* (2016), 2, pp. 120-127
[4] Karen, B., Analysis of Alternative Well-Control Methods for Dual-Density Deepwater Drilling, *Journal of Petroleum Technology*, *59* (2007), 1, pp. 61-63
[5] Mostafa, R. R., Managed-Pressure Drilling; Techniques and Options for Improving Operational Safety and Efficiency, *Petroleum and Coal*, *54* (2012), 1, pp. 24-33
[6] Xu, L., *et al*, Study on the Principle of Double Gradient Drilling Technology, *China Offshore Oil Gas (Engineering)*, *17* (2005), 4, pp. 260-264
[7] Hou, F., *et al*., Advances in Double-Gradient Drilling Technology for Subsea Pump Lifting, *China Petroleum Machinery*, *41* (2013), 6, pp. 68-71
[8] Lu, C., *et al*., Ultra-Deepwater Marine Double-Gradient Drilling Techniques, *Drilling Production Technology*, *24* (2001), 4, pp.25-27
[9] Jerome, J. S., *et al*., Well-Control Procedures for Dual Gradient Drilling as Compared to Conventional Riser Drilling, S*PE Drilling and Completion*, *21* (2006), 4, pp. 287-295
[10] Yang, Z., *et al.*, Development and Application of U-Shaped Tube Effect Controller, *Oil Drilling Production Technology*, *17* (1995), 5, pp. 26-29
[11] Zhou, Z., *et al*., Theoretical Study on the Effect of u-Tube on Variable Displacement Reduction of Cementing in Deep Wells, Science, *Technology and Engineering*, *9* (2009), 7, pp. 1863-1866
[12] Wellington, C., *et al.*, Free-Fall-Effect Calculation Ensures Better Cement-Operation Design, *SPE Drilling and Completion*, *8* (1993), 3, pp.175-178
[13] Ishii, M., *et al.*, *Thermo-Fluid Dynamics of Two-Phase Flow*, Springer Science and Business Media, Berlin, Germany, 2010

Appendix

Table 1. Well structure parameter

Depth [m]	Inside diameter [mm]
2493.3	245.37
5169	246.35
6511.8	266.7

Table 2. Liquid distribution inside the pipe and in the annulus parameter

Density [kgm^{-3}]	Yield stress [Pa]	Viscosity [Pa·s]	Liquidity index	Consistency coefficient [Pa·s^n]
2180	–3.27	0.089	0.91	48.85

Table 3. Tube combination parameter

	Inside diameter [mm]	Outside diameter [mm]	Length [m]	Number of drilling rod	Segment length [m]
Drilling Rod-1	129.9	149.2	5441	567	9.59612
Weighted drilling Rod-1	92.1	149.2	288	30	9.6
Drilling Rod-2	129.9	149.2	600	62	9.67742
Weighted drilling Rod-2	92.1	149.2	182.8	19	9.62105

Table 4. Liquid distribution table below the pipe column

	Density [kgm^{-3}]	Yield stress [Pa]	Viscosity [Pa·s]	Liquidity index	Consistency coefficient [Pa·s^n]
Drilling fluid	2180	–3.27	0.089	0.91	48.85

Table 5. Pressure parameter

Vertical depth [m]	Formation pressure [MPa]	Collapse pressure [MPa]	Leakage pressure [MPa]	Close pressure [MPa]	Fracturing pressure [MPa]
6008	108.336	111.869	0	125.411	146.02
6138	108.876	113.087	0	129.929	147.97
6192	104.372	112.261	0	131.072	148.67

Table 6. Injection fluid parameter

Name of liquid injected or operation successively	Volume [m^3]	Flow [m^{3}s^{-1}]	Continuous time
Isolation fluid-1	20	0.03	11:06
Cement paste-1	63	0.03	35:00
Pump-stop operation	–	–	10:00
Isolation fluid-2	5	0.03	2:46
Pump-stoped operation	–	–	5:00
Drilling fluid-1	23	0.03	12:46
Drilling fluid-2	5	0.03	2:46
Drilling fluid-3	10	0.03	5:33
Weighted drilling fluid-1	30	0.03	16:40
Weighted drilling fluid-2	3	0.02	2:30
Drilling fluid-4	11.5	0.02	9:35

Paper submitted: March 2, 2024
Paper revised: March 25, 2024
Paper accepted: May 15, 2024